

Piezoresistance effect in *p*-type Si

Y. Ohmura

Department of Electronic Engineering, Iwaki Meisei University, Iwaki, Fukushima 970, Japan

(Received 10 April 1990)

We present piezoresistance (PR) calculations of *p*-type Si, consistent with experimental ones, obtained from conductivity calculations for the sixfold valence band with and without stress. The small stress coefficients easily fulfill the symmetry requirement for the PR coefficients of the cubic crystal. From conductivity changes calculated separately for three heavy-hole, light-hole, and split-off band-derived bands, we conclude that the principal origin of PR in most cases is not the statistical redistribution but the mobility change of stress-deformed holes.

Since Smith¹ reported the piezoresistance (PR) effect in the cubic semiconductors Ge and Si, several theoretical works^{2,3} have been carried out on PR for *p*-type Si. However, no satisfactory interpretation to the whole effect has been given. The stress or strain effect on the valence-band structure has been clarified both theoretically^{4,5} and through low-temperature cyclotron resonance experiments.⁶ The quartet states at the top of the valence band decouple into two doubly degenerate states under the uniaxial stress. Near $\mathbf{k}=0$, the energy surfaces for two states are ellipsoids. The split-off band has a perturbing effect on the ellipsoids as the stress increases.

Gross features of the PR of the *p*-type Si are as follows. The longitudinal PR coefficients π_1 for $\langle 111 \rangle$ and $\langle 110 \rangle$ directions are large positive quantities, $\pi_1^{\langle 111 \rangle}$ being the largest. The $\pi_1^{\langle 001 \rangle}$ is positive but about an order of magnitude smaller than the former two. The transverse coefficients π_t for the above-mentioned three stress directions are negative quantities, $\pi_t^{\langle 001 \rangle}$ being the smallest. Large components usually have $(1/T)$ dependence near room temperature.⁷ Recently, nonlinear effects at high stress have also been observed.⁸

Theoretical works have hitherto attempted to explain these experimental data in terms of the above-mentioned stress-decoupled ellipsoids, where constant effective masses are assumed throughout the whole energy. However, ellipsoidal energy shapes are valid only near the band edges.⁹ In most energy regions, which are responsible for room-temperature conduction, energy shapes are quite different from ellipsoids. In this Brief Report, we show how incorporation of the exact *E-k* relation throughout the whole energy region necessarily leads to satisfactory interpretation of existing data.

The PR has been obtained from a conductivity¹⁰ for the sixfold valence band with and without stress,

$$\sigma = \sum_{i=1}^3 \sigma_i = \frac{ne^2}{4\pi^3 \hbar^2 k_B T} \sum_{i=1}^3 \int \tau \left[\frac{\partial \epsilon_i}{\partial k_c} \right]^2 f_0 d^3 k, \quad (1)$$

where the summation extends over three Kramers doublets $i=1, 2$, and 3 as arranged from the valence-band top. The integral and the derivative are replaced by a summation on $(171)^3$ points equally spaced in *k* space around $\mathbf{k}=0$ and a difference equation $(\Delta \epsilon_i / \Delta k_c)$, respectively, with the spacing $\Delta k = 25 \mu\text{m}^{-1}$ and the increment in the current direction $\Delta k_c = 1 \mu\text{m}^{-1}$. The Boltzmann distribution (f_0) and a constant relaxation time (τ) are assumed. The Fermi level η is determined by the hole concentration *n* as

$$\exp(-\eta/k_B T) = (1/4\pi^3 n) \sum_{i=1}^3 \int \exp(-\epsilon_i/k_B T) d^3 k. \quad (2)$$

The hole energy ϵ_i is obtained by a 6×6 DKK-type¹¹ *kp* Hamiltonian and strain Hamiltonian⁵ with $A = -4.22$, $B = -1$, and $N = -8.1$ (Ref. 12) in $(\hbar^2/2m_0)$ units and $D_u = 3.4$ eV and $D'_u = 4.4$ eV.¹³ The spin-orbit splitting between $J = \frac{3}{2}$ and $\frac{1}{2}$ states is taken as 44 meV.¹⁴ Stress is converted to strain with compliances $s_{11} = 0.768$, $s_{12} = -0.214$, and $s_{44} = 1.26$ in $10^{-12} \text{ cm}^2/\text{dyn}$.¹⁵ Calculated PR's are quite antisymmetric for an inversion from tensile to compressive stress of $1 \times 10^7 \text{ dyn/cm}^2$, from which PR coefficients are obtained. Table I shows PR coefficients for several stress (superscript) and current

TABLE I. Comparison of calculated and experimental piezoresistance coefficients in $10^{-12} \text{ cm}^2/\text{dyn}$ for 300 K.

$\pi_{\langle \text{current} \rangle}^{\langle \text{stress} \rangle}$	$\pi_{\langle 001 \rangle}^{\langle 001 \rangle} (\pi_{11})$	$\pi_{\langle 100 \rangle}^{\langle 001 \rangle} (\pi_{12})$	$\pi_{\langle 110 \rangle}^{\langle 110 \rangle}$	π_{44}	$\pi_{\langle 110 \rangle}^{\langle 110 \rangle}$	$\pi_{\langle 111 \rangle}^{\langle 111 \rangle}$	$\pi_{\langle 112 \rangle}^{\langle 111 \rangle}$
Calc.	5.4	-2.7	52.9	103.2	-50.2	68.8	-34.4
Expt.	6.6 ^a	-1.1 ^a	71.9 ^a	144 ^a		74 ^b	-38 ^b

^aReference 1.

^bReference 8.

(subscript) directions thus obtained for 300 K, together with experimental data. It should be noted that these coefficients almost perfectly meet the symmetry requirements of PR coefficients for the cubic crystal.¹⁶ Furthermore, π_{12} is nearly $-\pi_{11}/2$. The $\pi_{11} + 2\pi_{12}$ is the negative pressure coefficient of resistivity R_0 , $-(1/R_0)(dR_0/dp)$.¹ The above-mentioned valence-band structure used here is invariant for hydrostatic pressure, which may be the reason that π_{12} is nearly $-\pi_{11}/2$. Calculated large components agree fairly well with two kinds of data, and π_{11} reproduces Smith's data particularly well.

Next, we examine PR from the viewpoint of conductivity changes for three stress-split bands. Figure 1 shows piezoconductances (PC's) at 300 K for bands 1, 2, and 3 and the total one, from which PR is obtained, as a function of tensile (solid line) and compressive (dashed line) stresses for both the stress and the current parallel to the $\langle 111 \rangle$ direction. The PC's for bands 1, 2, and 3 are conductivity changes from those of the heavy-hole ($\sim 70\%$ of bulk), the light-hole ($\sim 25\%$), and the split-off band ($\sim 5\%$), respectively, which are normalized with bulk conductivity. Open symbols represent positive PC's and solid symbols represent negative ones. At the smallest stress of 1×10^7 dyn/cm², total PC's for both stresses stand close together, which is similar to antisymmetry of small-stress PR's for both stresses mentioned above. It is observed that even in each individual band, PC's for both stresses stand close together, however they gradually separate towards large stress. We will take notice of, say, PC (solid square) for tensile stress of 1×10^7 dyn/cm², which is the sum of a solid circle, a solid triangle, and an open inverse triangle for bands 1, 2, and 3, respectively. Thus, PC's for two lower hole-energy bands are negative. In a model of multivalleys with different mobilities, as the stress increases the conductivity for the lowest carrier-energy valley increases, but that for the higher-energy valley always decreases, which is due to the statistical redistribution of carriers.¹ Therefore, from this model, all the symbols for band 1 should be open (positive) and those for bands 2 and 3 should be solid (negative), since bands 2 and 3 go far from the top. The PC shown in Fig. 1 indicates that the principal origin of PR, at least for smaller stress, is not the statistical redistribution but may be a mobility change due to stress-deformed holes. At large stress, a sign reversal of PC (band 2 for compressive stress of $\sim 2 \times 10^9$ dyn/cm²) is observed. The reversal direction is that predicted by the above-mentioned constant-mobility multivalley model. In this figure for a combination of stress and current direction for the largest PR, it is found that the PC for band 1 is significantly large. Figure 2 shows differential conductivities normalized with bulk conductivity as a function of the hole energy for the stress and the current parallel to the $\langle 111 \rangle$ direction at a 3×10^9 dyn/cm² stress. It is observed that differential conductivities for both the tensile and the compressive stresses for band 1 are clearly resolved from that for the heavy hole and from each other because of large stress. Figure 3 shows densities of states for bands 1, 2, and 3 for the same case as in Fig. 2. It is observed that densities of states for the tensile and the compressive

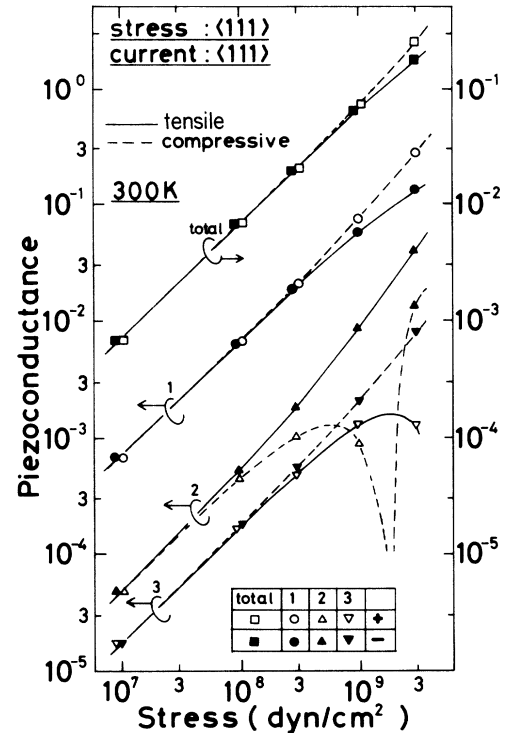


FIG. 1. Piezoconductances (PC's) for the total valence band and three bands as a function of tensile (solid line) and compressive (dashed line) stresses. Open symbols represent positive values and solid symbols represent negative values. Both the stress and the current are parallel to the $\langle 111 \rangle$ direction.

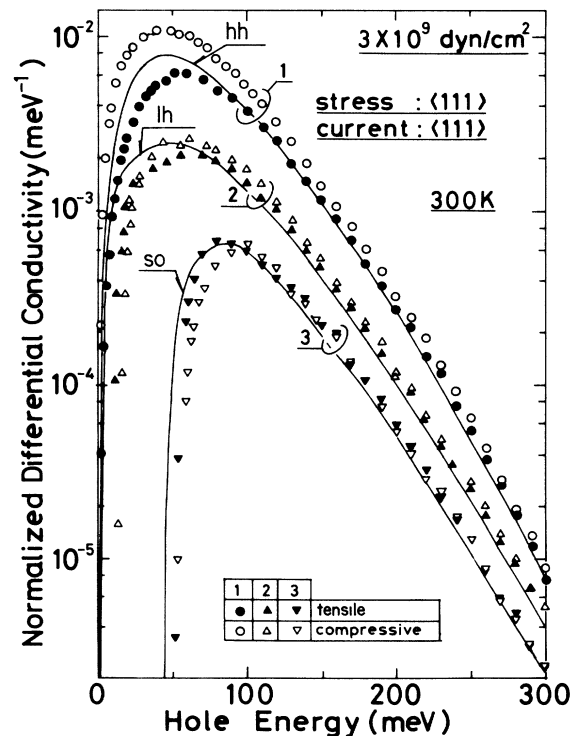


FIG. 2. Differential conductivities for three bulk bands and 1, 2, and 3 bands normalized with bulk conductivity for tensile (solid symbols) and compressive (open symbols) stresses of 3×10^9 dyn/cm² as a function of hole energy.

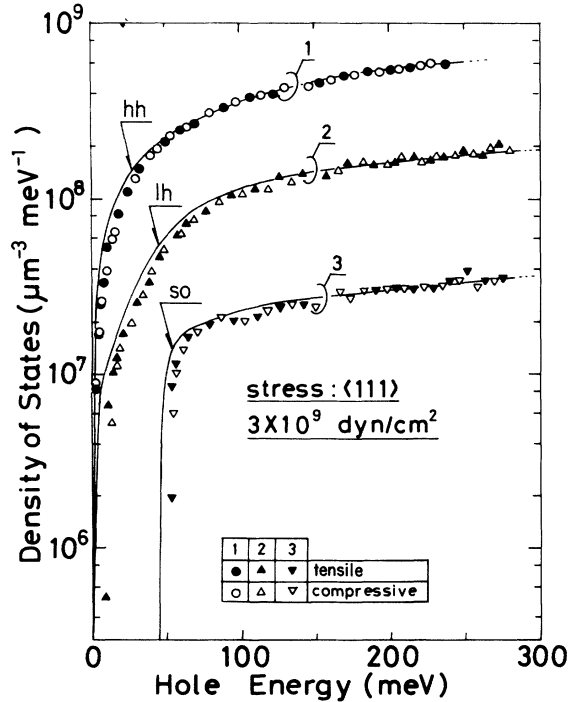


FIG. 3. Densities of states for three bulk bands and 1, 2, and 3 bands for tensile (solid symbols) and compressive (open symbols) stresses of $3 \times 10^9 \text{ dyn/cm}^2$ as a function of hole energy.

stresses for band 1 are almost similar to each other, although they are slightly smaller than that for the heavy hole at a small hole-energy region. This behavior in band 1 shown in Figs. 2 and 3 confirms the mobility change in band 1 carriers. Figure 4 shows a PC plot similar to Fig. 1 for a small component where both the stress and the current directions are parallel to the $\langle 001 \rangle$ direction. From the figure, it is found that the reason that PR for this case is an order of magnitude smaller than that for the case in Fig. 1 is the smallness of PC in band 1. The negative small PC in band 1 for tensile stress changes the sign to positive at $\sim 2 \times 10^9 \text{ dyn/cm}^2$, probably due to the statistical redistribution effect mentioned above. The PR shows a nonlinearity at large stress. For $\langle 111 \rangle$ stress, the second-order stress coefficients $\pi^{(2)}$ ($\langle 111 \rangle$ current) and $\pi^{(2)}$ ($\langle 11\bar{2} \rangle$ current) are $+6.8$ and $+35 \times 10^{-22} \text{ cm}^4/\text{dyn}^2$, respectively, which are in good agreement with experimental ones $+6.5$ and $27 \times 10^{-22} \text{ cm}^4/\text{dyn}^2$, respectively.⁸ The longitudinal PR

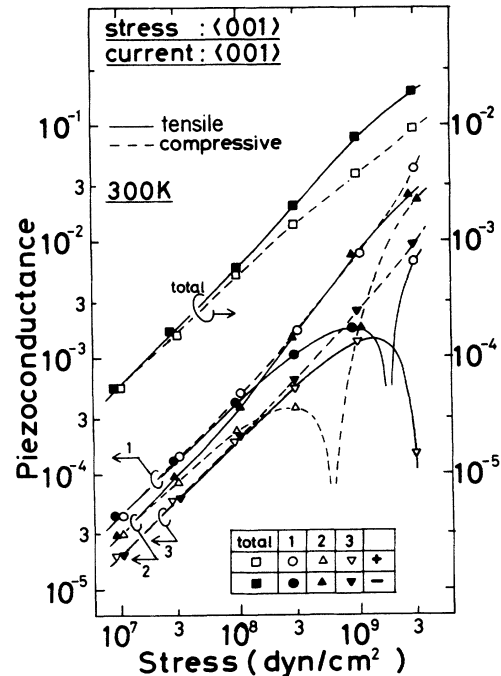


FIG. 4. PC's for the total valence band and three bands as a function of tensile (solid line) and compressive (dashed line) stresses. Open symbols represent positive values and solid symbols represent negative values. Both the stress and the current are parallel to the $\langle 001 \rangle$ direction.

coefficient for both the stress and the current parallel to the $\langle 110 \rangle$ direction starts from $52.9 \times 10^{-12} \text{ cm}^2/\text{dyn}$ at 300 K to $74.3 \times 10^{-12} \text{ cm}^2/\text{dyn}$ at 200 K , which is nearly a $1/T$ relation. However, it seems to saturate towards low temperature (114.3 at 100 K). This behavior is consistent with the experimental temperature dependence of this coefficient.⁷

In summary, we have calculated PR's of p -type Si that are consistent with experimental ones including large stress behavior and temperature dependence. The small stress PR coefficients well meet the symmetry relationships. We suggest that the mobility change of stress-deformed holes is the principal origin of PR.

The author gratefully acknowledges the Iwaki Meisei University Computer Center (IMUCC). He would like to thank T. Hanzawa, H. Takayama, and T. Ishikawa for their kind advice in TSS FORTRAN programming.

¹C. S. Smith, Phys. Rev. **94**, 42 (1954).

²G. E. Pikus and G. L. Bir, Fiz. Tverd. Tela (Leningrad) **1**, 154 (1959) [Sov. Phys.—Solid State **1**, 136 (1959)].

³K. Suzuki, H. Hasegawa, and Y. Kanda, Jpn. J. Appl. Phys. **23**, L871 (1984).

⁴G. E. Pikus and G. L. Bir, Phys. Rev. Lett. **6**, 103 (1961).

⁵H. Hasegawa, Phys. Rev. **129**, 1029 (1963).

⁶J. C. Hensel and G. Feher, Phys. Rev. **129**, 1041 (1963).

⁷F. J. Morin, T. H. Geballe, and C. Herring, Phys. Rev. **105**, 525 (1957).

⁸K. Yamada, M. Nishihara, S. Shimada, M. Tanabe, and M. Shimazoe, Trans. IEE Jpn. **103-A**, 555 (1983) (in Japanese).

⁹Y. Ohmura, J. Phys. Soc. Jpn. **47**, 145 (1979).

¹⁰For example, F. J. Blatt, in *Solid State Physics*, edited by F. Seitz and D. Turnbull (Academic, New York, 1957), Vol. 4.

¹¹G. Dresselhaus, A. F. Kip, and C. Kittel, Phys. Rev. **98**, 368

- (1955).
- ¹²J. J. Stickler, H. J. Zeiger, and G. S. Heller, *Phys. Rev.* **127**, 1077 (1962).
- ¹³I. Balslev and P. Lawaetz, *Phys. Lett.* **19**, 6 (1965).
- ¹⁴S. Zwerdling, K. J. Button, B. Lax, and L. M. Roth, *Phys. Rev. Lett.* **4**, 173 (1960).
- ¹⁵J. J. Wortman and R. A. Evans, *J. Appl. Phys.* **36**, 153 (1965).
- ¹⁶W. G. Pfann and R. N. Thurston, *J. Appl. Phys.* **32**, 2008 (1961).